Wind Fields From C- and X-Band SAR Images at VV Polarization in Coastal Area (Gulf of Oristano, Italy)

SUBMISSION DATE / POSTED DATE

11-07-2023 / 25-07-2023

CITATION

zecchetto, stefano; De Biasio, Francesco; della Valle, Antonio; Quattrocchi, Giovanni; Cadau, Enrico; Cucco, Andrea (2023). Wind Fields From C- and X-Band SAR Images at VV Polarization in Coastal Area (Gulf of Oristano, Italy). TechRxiv. Preprint. https://doi.org/10.36227/techrxiv.23661195.v1

DOI

10.36227/techrxiv.23661195.v1

Wind Fields from C and X band SAR images at VV polarization in coastal area (Gulf of Oristano, Italy)

Stefano Zecchetto, Francesco De Biasio, Antonio della Valle, Andrea Cucco, Giovanni Quattrocchi and Enrico Cadau

***Abstract*—This work deals with the spatial characteristics of the wind fields evaluated from Synthetic Aperture Radar (SAR) images and simulated by the Weather Research and Forecasting (WRF) atmospheric model in the Gulf of Oristano, a small coastal area about 10 km by 18 km wide in western coast of Sardinia (Western Mediterranean Sea). The SAR derived wind fields have been obtained analyzing images of the COSMO-SkyMed, Radarsat-2 and Sentinel-1A satellites through a fully two-dimensional continuous wavelet method (2D-CWT). The analysis of the wind directions has shown that the model variability is limited if compared with that inferred by 2D-CWT method, which mostly respects the variability evidenced by in-situ data. As the use of model directions to compute the SAR wind fields is a standard in many studies, the impact on the SAR wind speed retrieval of using the model instead of the SAR derived directions has been assessed: differences of wind speed greater than $\pm 10\%$ occur for about the 20% of data. The spatial variability of the SAR and model wind speed fields results quite different at both local and domain scale. The knowledge of the spatial variations of the surface wind fields can be very important for the oceanographic applications and constitutes the added value brought by SAR in the description of the coastal wind. For this reason the SAR derived wind fields should be taken as reference in many kind of applications.**

***Index Terms*—SAR, COSMO-SkyMed, Radarsat-2, Sentinel-1A, coastal meteorology, surface wind.**

I. Introduction

COASTAL sea areas, roughly extending in the internal waters (up to ≈20 km from the coast), at present are not sensed by satellite scatterometers providing wind data. For instance, the Meteorological Operational satellites (MetOp) do not provide data closer than 15 km from coast [1]. Due to the interaction between the wind flow and the orography, the winds in coastal areas are often not well reproduced by both global and regional atmospheric models [2], [3]. Therefore, the possibility to derive the surface wind field from Synthetic Aperture Radar (SAR) images is extremely important because it could provide a deeper knowledge of the spatial characteristics of the wind. This aspect is particularly relevant considering that the wind fields from atmospheric numerical models, which are generally used to force the three-dimensional hydrodynamic numerical models, are hardly validated due to the lack of in-situ winds observations both along coast and offshore.

In coastal areas, the short term prediction of the main hydrodynamics parameters such as the sea temperature and salinity, water currents, wind wave height by means of numerical modeling techniques is strongly sensitive to the spatial and temporal variability of the wind.

At present, the SAR is the only satellite sensor providing information of the spatial variability of the wind over the sea: just looking to a SAR radar backscatter image, an experienced eye is able to infer qualitatively the areas where the wind is stronger and often, looking to the backscatter signatures layout, to infer also the wind direction. However, moving from a qualitative to a quantitative approach is far to be easy, as the techniques to estimate the wind field from SAR are not fully reliable yet, despite several published works [4]–[10]. Furthermore, even if established methodologies were available, the exploitation of the SAR derived winds in coastal context would remain, in our opinion, an open question, basically because their poor re-visitation time at middle latitudes. The SAR derived winds are used to map coastal areas for wind energy resources [11]–[13], to study up-welling oceanographic occurrence [14] and have been assimilated into atmospheric models [15].

In this paper we show and discuss three examples of SAR derived winds in the Gulf of Oristano, obtained from three different satellites. The main purpose is to evidence the spatial characteristics of the SAR derived winds with respect to those from a regional atmospheric model, to emphasize again what it is well known about the detailed descriptions of the wind fields provided by SAR. The starting point of this work is the known difficulty of atmospheric models to describe the local characteristics of the wind fields in the coastal regions [2], [3], because often their spatial scales are smaller than the model grid size. Therefore, this work is aimed to a) discuss the characteristics of the SAR derived wind speed and direction in comparison with those from the atmospheric model and b) to investigate the potential errors in the SAR wind speed determination, introduced by using external wind direction information as those from atmospheric models. We talk here on "potential errors" since our data set of only three images does not permit to achieve statistically robust results, but rather to indicate the sources and amount of the discrepancies.

It is structured as follows: section II describes the area of interest, the wind network operating here and introduces the atmospheric model used; section III describes the SAR images used to derive the wind field through the technique outlined in section IV. Results, discussed separately in terms of wind direction and speed, are given in section V. Section VI is devoted to discussion and conclusions.

S. Zecchetto, F. De Biasio and A. della Valle are with the Istituto Scienze dell' Atmosfera e del Clima, Padova, Italy e-mail: stefano.zecchetto@cnr.it

A. Cucco and G. Quattrocchi are with the Institute for Coastal Marine Environment,National Research Council of Italy, Oristano, Italy

E. Cadau is with Sardegna Clima Onlus, Fonni, Italy

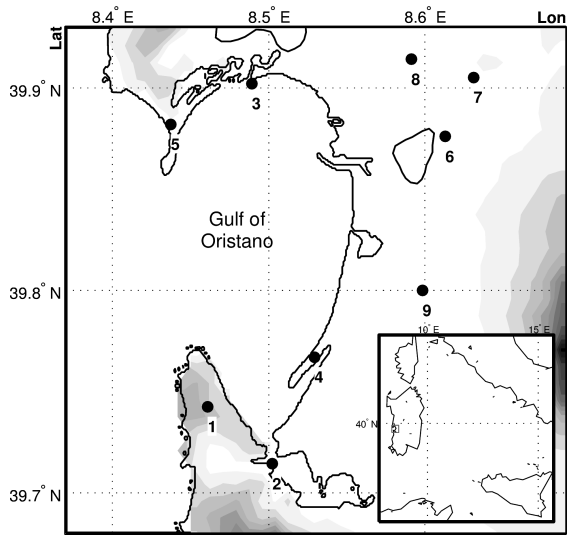

Fig. 1. Map of the Gulf of Oristano with the positions of the stations. The gray shadows indicate the elevation with a step of 20 m. The black dots indicate the experimental wind stations.

II. The area of interest

The Gulf of Oristano (Fig. 1) is a shallow water, semi-enclosed bay, located along the western coast of Sardinia island (Western Mediterranean Sea). It is about 10 km by 18 km wide, surrounded by salt marshes and lagoon systems connected to the Gulf through complicated nets of natural and artificial channels. The average water depth is about 16 m. The Gulf is bounded on the north and south by two capes which, with the altitudes of about 60 and 80 meters, are the highest reliefs in the surroundings. The area is mainly subject to winds from north-west (mistral, $\approx$ 43 %) and from south-east (sirocco, $\approx$ 18 %), according to the statistics obtained from almost sixteen years of scatterometer wind data (2000-2015). The Gulf of Oristano is an important site for local fishery, aquaculture and recreational activities, most of them carried out along the coastline and inside the surrounding lagoons. To provide a support to these economical activities, several numerical applications were developed during the last decades, including hydrodynamic [16], wind wave [17] and water quality models [18].

In the area, a Wind Measuring System (WMS) (Fig. 1) has been realized to support the hydrodynamic and ecological numerical applications [19]. It consists of five three-components anemometers (sites 1-5) all except one located along the coast few meters from the sea at heights between 2 m and 10 m from the ground (sites 2-5), plus four standard cup anemometers located inland (few kilometers from coast, sites 6-9, belonging to the weather network of Sardegna Clima Onlus). The acquisition is continuous since 2014: every hour, data from the wind system are downloaded, processed and published on the web[1].

Meteorological hindcasts have been carried out with the Weather Research and Forecasting (WRF) model [20], version 3.6.1, in a configuration summarized in Table I.

[1]http://www.sardegna-clima.it/index.php/vento-golfo-oristano

Model version	3.6.1
Domains	3
Horizontal resolution	7.2, 2.4, 0.8 km
Vertical resolution	40 levels
Input data	Analysis and forecast by ECMWF
Nesting	2-way nesting
Physic schemes	
Microphysics	WSM6 [21]
long-wave	RRTM [22]
short-wave	Dudhia [23]
Cumulus	Kain-Fritsch [24]
LSM	Noah scheme [25]
PBL+SL	ACM2 [26]

TABLE I
WRF MODEL CONFIGURATION USED.

The performances of WRF over the sea have been discussed in [27]–[31]. Wind speed and directions at 10 m of reference height from one year of WRF simulations have been compared with the experimental data (reported at 10 m of reference height using a boundary layer model based from the Monin-Obukhov theory [32]), indicating a mean WRF underestimate of wind speed of 3% with a RMSE of 2.2 ms^{-1} and a negligible wind direction bias of 5 degrees with a RMSE of 37 degrees. These values are encouraging, but do not prevent large differences, as indicated by the high values of RMSE. The activity of WRF validation in the Gulf of Oristano is ongoing.

III. The SAR images

The SAR images presented in this work are from the following satellites: COSMO-SkyMed (CSK) of the Italian Space Agency [33], Radarsat-2 (RS2) of the Canadian Space Agency [34] and Sentinel-1A (S1A) of the European Space Agency [35], all at VV polarization. The CSK image is a Stripmap Himage; the RS2 a Scansar Narrow image; the Sentinel-1A a level 1 High Resolution (HR) Ground Range Detected (GRD) Interferometric Wide swath (IW) image. Their main characteristics, along with the mean environmental conditions at the satellite pass time, are reported in Table II. The images, radiometrically calibrated [36]–[38] with the Sentinel Application Platform v2.0 software (SNAP, http://step.esa.int/main/toolboxes/snap/), are shown in Fig. 2 with the in-situ wind vectors superimposed.

Satellite	CSK	RS2	S1A
Image type	Stripmap Himage	Scansar Narrow	HR-GRD-IW
Date	1 Apr 2015	23 Jun 2014	3 Apr 2015
Time (GMT)	05:12	17:17	05:28
Band	X	C	C
Orbit	ascending	ascending	descending
Polarization	VV	VV	VV
Pixel in range m	1.3	25	10
Pixel in azimuth m	2.1	25	10
wind speed (ms^{-1})	7.4	5.9	5.0
wind direction (°)	309	146	314
$T_{air} - T_{sea}$ (°C)	-0.5	7.2	-0.8

TABLE II
MAIN CHARACTERISTICS OF THE IMAGES USED IN THIS WORK AND THE GEOPHYSICAL CONDITIONS FROM THE EXPERIMENTAL DATA.

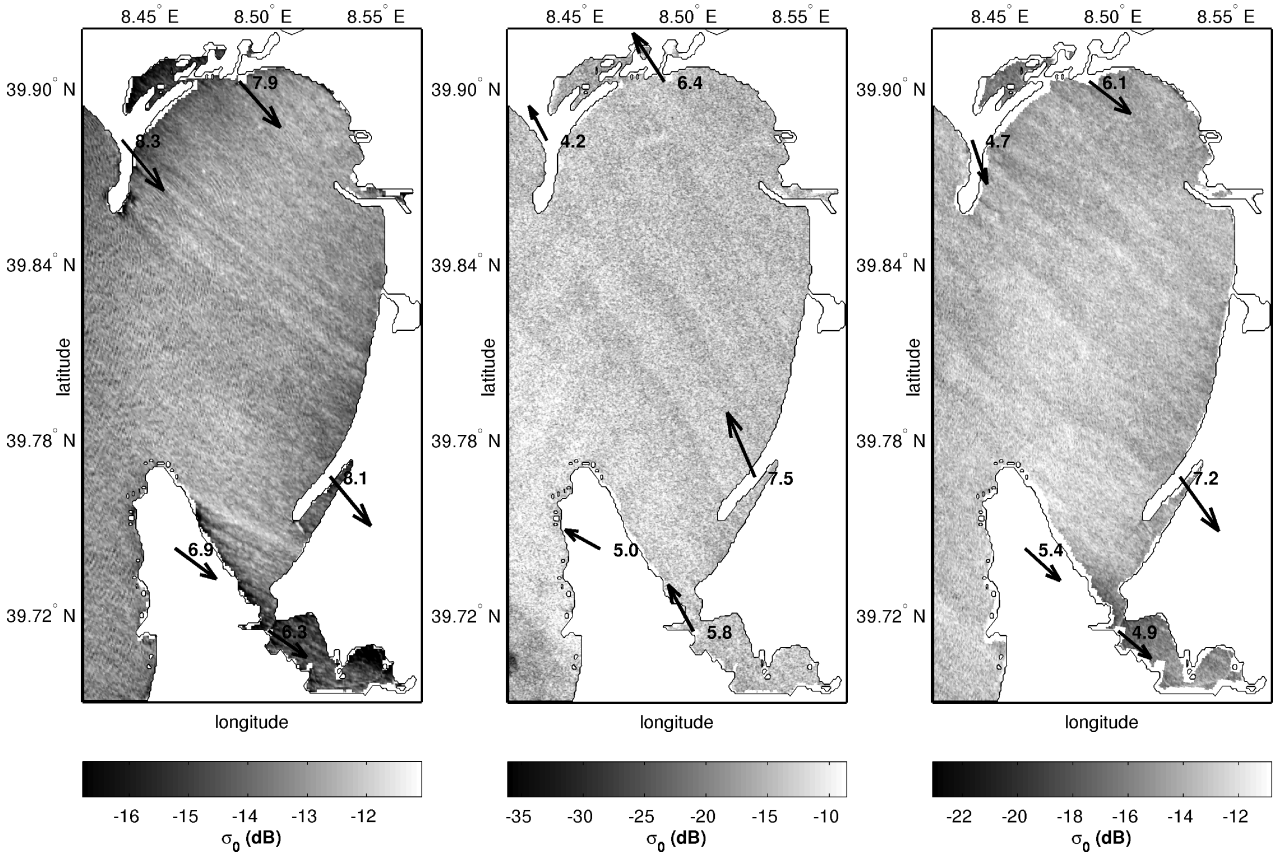

Fig. 2. The SAR images with the experimental winds superimposed. Left panel: COSMO-SkyMed image, 1 April 2015, 05:12 GMT, X band, VV pol (COSMO-SkyMed Product - ©ASI - Agenzia Spaziale Italiana - (2015). All Rights Reserved). Middle panel: Radarsat-2 image, 23 June 2014 17:17 GMT, C band, VV pol (RADARSAT-2 Data and Products - © MacDonald, Dettwiler and Associates Ltd. (2014). All Rights Reserved. RADARSAT is an official trademark of the Canadian Space Agency). Right panel: Sentinel-1A HR-GDR-IW, C band, VV pol (3 April 2015, 05:28 GMT).

All images were taken under moderate wind conditions: the CSK and S1A (left and right panels) under northwest wind of about 7 ms^{-1}, the RS2 (middle panel) under southeast wind of about 6 ms^{-1}. The air-sea stability conditions were near neutral for CSK and S1A, strongly stable for RS2 (Table II). Due to their high spatial resolution, all images evidence several geophysics phenomena, such as sea gravity waves, wind rolls and wind shading areas close to coast. Such richness of details results very challenging for any methodology aimed to extract the wind direction, since the complex texture of the radar backscatter.

IV. The Method to Extract the Wind Direction from SAR

To derive the wind field from SAR images, it is necessary to know the wind direction, which may be taken from atmospheric models [8] or derived from the SAR signatures [5], [6], [9], [10]. To estimate the wind directions over the sea area we have refined the 2D Continuous Wavelet Transform (2D-CWT) technique described in [7], [10] by using a two dimensional, directional Morlet mother wavelet, chosen because its definite relationship between dilation scales and wave numbers: this permits to define the scales length on a geophysical basis and to convert them to dimensionless dilation scales for the computation (see [39]–[41] for introduction of the Continuous Wavelet Transform).

Without entering into details, it suffices here to say that our method is based on: a) the computation of the wavelet 2-D spectrum of SAR image to find the spatial scales and the directions where the energy related to the wind speed is located; b) the reconstruction a SAR-like image only with selected scales and angles to evidence the shape of the backscatter structures related to the wind; c) the analysis of the shape of these structures (wind cells) to get the direction of their major axis. This is taken as the wind direction with 180° of ambiguity. The geophysical scales investigated are from 200 m to 900 m, the scales of the wind signatures [7], [10], the angles from 0 to π at steps of $\pi/18$. The mean wind cell radar backscatter has been then obtained averaging all the wind cells: its spatial structure results asymmetric with respect to the cell major axis. This asymmetry has been used to resolve the 180° direction ambiguity (de-aliasing). Details may be found in [10]. Of course this technique, as all those retrieving the wind direction from the SAR radar backscatter, needs the presence of well defined signatures in the image to be successful: therefore it works better under high than under low winds. Once determined the wind direction of each wind cell, the wind speed has been computed using the CMOD5 model [42] for Radarsat-2 and Sentinel-1A (C-band) and the XMOD2, developed for the TerraSAR-X satellite [43], for COSMO-SkyMed (X-band).

Figure 3, obtained from the analysis of the CSK image, shows the wind cells, broadly aligned to the wind directions of the in-situ data indicated by the arrows. Note, however, the direction variability in all the domain and along coast.

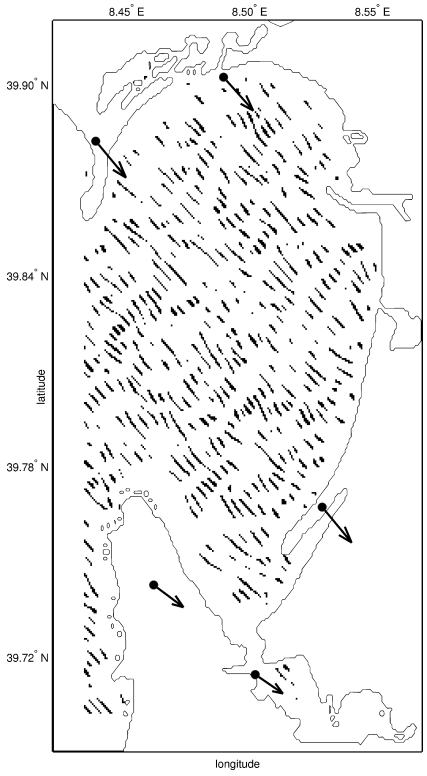

Fig. 3. The wind cells detected by the 2D-CWT analysis of the CSK image of Fig. 2. The vectors indicate the experimental wind.

V. RESULTS

A. Wind direction

The wind fields resulting from the 2D-CWT analysis (hereafter referred as SAR winds) are shown in the top panels of Fig. 4: they are unevenly spaced because they follow the location of the detected wind cells. In all the three cases, the wind direction fields appear spatially variable, a feature absent in the corresponding WRF fields (Fig. 4, bottom panels) which are much more smoothed. This is a well known characteristic of the numerical modeling (see [3] and the references quoted there). Table III reports the mean characteristics of the wind direction at the experimental site locations, obtained from the in-situ reports, from the SAR and the WRF wind fields. The experimental values have been obtained averaging the data within a time window $\pm$ 200 seconds the satellite pass time; those of the fields averaging the vectors located inside a circle with radius of 0.03°, about 3 km, centered on the experimental sites. The choice of these numbers is based on the Taylor principle of frozen turbulence [44]. The mean directions of the SAR wind fields are very close to both the experimental and WRF values, with differences smaller than 6°. The direction variability, expressed by the standard deviation, appears well reproduced by the SAR wind, close to that derived from the experimental data. On the contrary, WRF reports a much smaller variability, reflecting the smooth characteristics of its fields.

	CSK	RS2	S1A
Site	309±10	146±8	314±12
SAR	315±8	145±12	309±10
WRF	312±2	147±3	310±2

TABLE III
STATISTICS OF THE WIND DIRECTION. VALUES IN DEGREES.

Of course, it is not possible to say which representation of the wind direction field is closer to reality, as experimental observations are not available in the locations of the SAR and model winds. However, the fact that the SAR wind shows a directional variability closer to the experimental data and higher than WRF, supports the convenience of estimating the wind direction directly from the SAR images, as done by the 2D-CWT method, and justifies our general warning that the use of model wind directions to derive the SAR wind field can be inadvisable in coastal areas. This recommendation is supported by the results reported in [45].

B. Wind speed

To be compared with the WRF winds, the SAR wind fields have been recomputed over the WRF grid, interpolating the SAR wind directions on the grid points and averaging the radar backscatter around each grid point. The mean characteristics of the wind speeds at the in-situ locations, computed as those of the wind direction, are shown in Table IV: again we notice similar wind speed variability, expressed by the standard deviation, for SAR and experimental data, while that of WRF is lower. The SAR derived mean speed is close to the measured value only for RS2, while for CSK and S1A it results higher. While for CSK we may guess that this is due to the model function used (XMOD2 has been developed for TerraSAR-X satellite), the discrepancy of S1A is unexpected, because it operates at C-band and its radiometric calibration of 0.67±0.45 dB, given in [37], is good. However, this bias does not hinder our discussion focused on the spatial variability of the winds, rather than on their mean strength.

	CSK	RS2	S1A
Site	7.4±1.0	5.9±1.0	5.0±0.7
SAR	8.9±1.2	5.1±1.0	9.3±1.3
WRF	7.3±0.5	7.7±0.4	5.7±0.3

TABLE IV
STATISTICS OF THE WIND SPEED. VALUES IN ms^{-1}.

Figure 5 reports the wind speed fields, from SAR (top panels) and WRF (bottom panels). The patterns of the wind speed variability exhibited by the SAR fields appear very detailed, and WRF is able to catch only the large scale features, such as the north-south gradient for S1A (right panels) and some areas of lower wind in the RS2 (middle panels). In the case of the CSK case, the patterns are totally different, indicating that also the most sophisticated atmospheric models may produce, at local scale, unreliable results.

VI. Discussion and conclusion

An accurate determination of the wind direction is important for many reasons: first of all because of its influence on the computation of the wind speed from SAR; then for all the applications related to the sea surface transport such as, for instance, the monitoring of the sea surface pollutants and of the presence/absence of alloctone/aliens species in coastal areas. Furthermore, the wind direction is crucial in the determination of the wind relative vorticity, important to understand many features of the wind field and several permanent or semi permanent oceanographic phenomena [46]. In the following we discuss the first aspect.

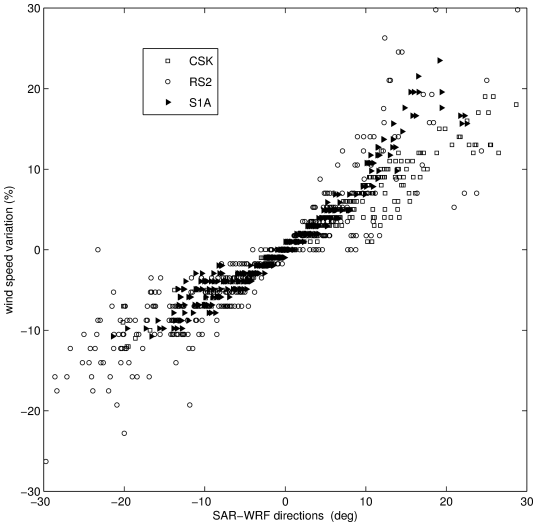

Fig. 6. Percent variations of the wind speed using external wind direction (WRF directions in this case) in place of the SAR derived direction, as a function of the SAR-WRF wind direction difference for the three images analyzed.

The retrieved SAR wind speed can be substantially different using different wind directions. Figure 6 shows the percent change of the wind speed using the WRF instead of the SAR wind directions, i.e. $100 < (w_{sar} - w_{wrf})/w_{sar} >$, where w_{sar} and w_{wrf} are the wind speed obtained using SAR and WRF wind directions respectively, and $<>$ the spatial mean, as a function of the SAR-WRF wind direction difference. Differences greater than $\pm 10\%$ are fairly frequent ($\approx 20\%$ of data) for the three cases analyzed, large enough to consider important this issue and to continue this kind of analysis investigating the geophysical impacts of such a differences. Their spatial layout obviously reflects that of the wind direction difference between the model and the SAR derived direction (not shown).

They may be due to two factors: the bias between the directions (in this case very small) and the direction variability discussed in Section V. In our knowledge, these aspects have been neglected in literature and should be at least mentioned when SAR derived wind fields are presented, as the reliability of the wind direction has a direct impact of the determination of wind speed. Reliable means a) directions reproducing the mean wind flow and b) directions reproducing the natural variability of the wind direction. Despite the small data set of SAR images, the 2D-CWT technique used to extract the wind directions without any external information provides reliable wind direction estimates, both in terms of mean flow and of wind direction variability. This has been achieved using different kinds of SAR data, with different spatial resolutions and microwave frequencies. We have also shown how the wind directions may impact on the determination of the SAR wind speed.

A second important issue concerns the representation of the wind fields provided by SAR and WRF model, revealing fields with different spatial features. This point is very important, because it enlightens the potentialities of using the SAR derived wind fields in coastal areas. The spatial layout of the wind field is important for oceanographic applications, as those related to the numerical reproduction of the water circulation, and this is the reason why we stress this point.

Summarizing, the results of the 2D-CWT are encouraging: the wind directions extracted from the SAR images are very close to those measured both in terms of mean and variability. This assures a correct determination of the SAR wind fields, which however appear very different, in strength and spatial layout, from those modeled, providing a warning about the capability of the atmospheric models to describe the wind field over small coastal areas and consequently rising the question about their use in the determination of the wind field from SAR. The wealth of information brought by the SAR derived wind fields suggests to take them as reference in any kind of application.

Acknowledgment

This work has been supported by the project *RITMARE, (www.ritmare.it)* funded by the Italian Ministry of University and Research. The Cosmo-SkyMed and Radarsat-2 SAR images have been obtained in the framework of the COSMO-SkyMed/RADARSAT-2 Initiative of the Italian Space Agency and the Canadian Space Agency *Ocean wind fields from C and X-band SAR in the coastal areas*, Proposal id 2868/5224. The project is carried out using CSK (©ASI - Agenzia Spaziale Italiana - (2015). All Rights Reserved) delivered under an ASI license and RADARSAT-2 Data and Products images (© MacDonald, Dettwiler and Associates Ltd. (2014). All Rights Reserved. RADARSAT is an official trademark of the Canadian Space Agency). The Sentinel-1 image has been downloaded from the ESA Sentinels Scientific Data Hub (https://scihub.copernicus.eu/). The Authors wish to thank the two anonymous referees for their stimulating review.

References

[1] OSISAF, "ASCAT Wind Product User Manual (Ver. 1.12)," Eumetsat, Darmstadt, Germany, Tech. Rep. SAF/OSI/CDOP/KNMI/TEC/MA/126, August 2012, available online at http://www.knmi.nl.

[2] C. Accadia, S. Zecchetto, A. Lavagnini, and A. Speranza, "Comparison of 10-m Wind Forecasts from a Regional Area Model and QuikSCAT Scatterometer Wind Observations over the Mediterranean Sea," *Monthly Weather Review*, vol. 135, pp. 1946–1960, 2007.

[3] S. Zecchetto and C. Accadia, "Diagnostics of T1279 ECMWF analysis winds in the Mediterranean Basin by comparison with ASCAT 12.5 km winds," *Quarterly Journal of the Royal Meteorological Society*, 2014.

[4] C. Wackerman, C. Rufenach, R. A. Shuchman, J. Johannessen, and K. Davidson, "Wind vector retrieval using ERS-1 Synthetic Aperture Radar imagery," *IEEE Trans. Geos. and Remote Sensing*, vol. 34, pp. 1343–1352, 1996.

[5] S. Lehner, J. Horstmann, W. Koch, and W. Rosenthal, "Mesoscale wind measurements using recalibrated ERS SAR images," *J. Geophys. Res*, vol. 103, pp. 7847–7856, 1998.

[6] Y. Du, P. W. Vachon, and J. Wolfe, "Wind direction estimation from SAR images of the ocean using wavelet analysis," *Canadian Journal of Remote Sensing*, vol. 28, no. 3, pp. 498–509, 2002.

[7] S. Zecchetto and F. De Biasio, "On shape, orientation and structure of atmosheric cells inside wind rolls in two SAR images ," *IEEE Trans. of Geoscience and Remote Sensing*, vol. 40, no. 10, pp. 2257–2262, 2002.

[8] F. M. Monaldo, D. R. Thompson, W. G. Pichel, and P. Clemente-Colon, "A Systematic Comparison of QuikSCAT and SAR Ocean Surface Wind Speeds," *IEEE Trans. Geoscience and Remote Sensing*, vol. 42, no. 2, 2004.

[9] W. Koch and F. Feser, "Relationship between SAR-Derived Wind Vectors and Wind at 10-m Height Represented by a Mesoscale Model," *Monthly Weather Review*, vol. 134, pp. 1505–1517, 2006. [Online]. Available: http://dx.doi.org/10.1175/MWR3134.1

[10] S. Zecchetto and F. De Biasio, "A Wavelet Based Technique for Sea Wind Extraction from SAR Images," *IEEE Trans. of Geoscience and Remote Sensing*, vol. 46, no. 10, pp. 2983–2989, 2008.

[11] M. B. Christiansen, W. Koch, J. Horstmann, C. B. Hasager, and M. Nielsen, "Wind resource assessment from C-band SAR," *Remote Sensing of Environment*, vol. 98, no. 2-3, pp. 251–268, 2006.

[12] C. B. Hasager, M. Badger, A. Peña, X. G. Larsen, and F. Bingöl, "SAR-Based Wind Resource Statistics in the Baltic Sea," *Remote Sens.*, vol. 3, no. 1, pp. 117–144, 2011.

[13] R. Chang, R. Zhu, M. Badger, C. B. Hasager, R. Zhou, D. Ye, and X. Zhang, "Applicability of Synthetic Aperture Radar Wind Retrievals on Offshore Wind Resources Assessment in Hangzhou Bay, China," *Energies*, vol. 7, p. 2014, 3339-3354.

[14] T.-S. Kim, K.-A. Park, X. Li, and S. Hong, "SAR-derived wind fields at the coastal region in the East/Japan Sea and relation to coastal upwelling," *International Journal of Remote Sensing*, vol. 35, no. 11-12, pp. 3947 – 3965, 2014.

[15] B. R. Furevik, K. F. Dagestad, G. Noer, and P. Jaccard, "Use of SAR winds in marine weather forecasting," in *Proceedins of IGARSS2015*. Milan, Italy, 26-31 July, 2015.

[16] A. Cucco, A. Perilli, G. De Falco, M. Ghezzo, and G. Umgiesser, "Water circulation and transport timescales in the Gulf of Oristano," *Chemistry and ecology*, vol. 22, pp. 307–331, 2006.

[17] G. De Falco, M. Baroli, A. Cucco, and S. Simeone, " Intrabasinal conditions promoting the development of a biogenic carbonate sedimentary facies associated with the seagrass Posidonia oceanica," *Continental Shelf Research*, vol. 28, no. 6, pp. 797–812, 2008.

[18] A. Cucco, M. Sinerchia, A. Ribotti, A. Olita, L. Fazioli, A. Perilli, B. Sorgente, M. Borghini, K. Schroeder, and R. Sorgente, "A high-resolution real-time forecasting system for predicting the fate of oil spills in the Strait of Bonifacio (western Mediterranean Sea)," *Marine Pollution Bulletin,*, vol. 64, no. 6, pp. 1186–1200, 2012.

[19] S. Zecchetto, A. Della Valle, F. De Biasio, G. Quattrocchi, E. Cadau, and A. Cucco, "The wind measuring system in the Gulf of Oristano as support to the regional scale oceanographic modeling," *Journal of Operational Oceanography*, vol. in press, 2015.

[20] W. Skamarock, J. Klemp, J. Dudhia, D. Gill, D. Barker, M. Duda, X. Huang, W. Wang, and J. Powers, "A description of the advanced research WRF version 3," NCAR Technical Note, Tech. Rep. NCAR/TN-475+STR, 2008.

[21] S. Hong and J. Lim, "The WRF Single-Moment 6-Class Microphysics Scheme (WSM6)," *J. Korean Meteor. Soc.*, vol. 42, no. 2, pp. 129–151, 2006.

[22] E. Mlawer, S. Taubman, P. Brown, M. Iacono, and S. Clough, "Radiative transfer for inhomogeneous atmospheres: RRTM, a validated correlated-k model for the longwave," *J. of Geophysical Research*, vol. 102, no. D14, pp. 16 663–16 682, 1997.

[23] J. Dudhia, "Numerical Study of Convection Observed during the Winter Monsoon Experiment Using a Mesoscale Two-Dimensional Model," *J. Atmos. Sci.*, vol. 46, no. 20, pp. 3077–3107, 1989.

[24] J. Kain, "The Kain–Fritsch convective parameterization: an update," *J. Appl. Meteor.*, vol. 43, pp. 170–181, 2004.

[25] F. Chen and J. Dudhia, "Coupling an Advanced Land Surface Hydrology Model with the Penn State NCAR MM5 Modeling System. Part I: Model Implementation and Sensitivity," *Monthly Weather Review*, vol. 129, pp. 569–585, 2001.

[26] J. Pleim, "A Combined Local and Nonlocal Closure Model for the Atmospheric Boundary Layer. Part II: Application and Evaluation in a Mesoscale Meteorological Model," *Journal of Applied Meteorology and Climatology*, vol. 46, no. 9, pp. 1396–1409, 2007.

[27] S. Shimada and K. Ohsawa, "Accuracy and characteristics of offshore wind speeds simulated by WRF," *SOLA*, vol. 7, pp. 21–24, 2011.

[28] D. Carvalho, A. Rocha, M. Gomez Gesteira, and C. Silva Santos, "Sensitivity of the WRF model wind simulation and wind energy production estimates to planetary boundary layer parameterizations for onshore and offshore areas in the Iberian Peninsula," *Applied Energy*, vol. 135, pp. 234–246, 2014.

[29] M. Menendez, M. García-Díez, L. Fita, J. Fernández, F. Méndez, and J. Gutiérrez, "High-resolution sea wind hindcasts over the Mediterranean area," *Climate Dynamics*, vol. 42, no. 7-8, pp. 1857–1872, 2014.

[30] E.-M. Giannakopoulou and R. Nhili, "WRF Model Methodology for Offshore Wind Energy Applications," *Advances in Meteorology*, vol. 2014, pp. 1–14, 2014, article ID 319819.

[31] S. Vishnu and P. A. Francis, "Evaluation of high-resolution WRF model simulations of surface wind over the west coast of India," *Atmospheric and Oceanic Science Letters*, vol. 7, no. 5, pp. 458–463, 2014.

[32] A. S. Monin and A. M. Obukhov, "Basic laws of turbulent mixing in the ground layer of the atmosphere," *Tr. Akad. Nauk SSSR Geofiz. Inst.*, vol. 24 (151), pp. 163–187, 1954.

[33] Agenzia Spaziale Italiana (ASI), *COSMO-SkyMed System Description&User Guide*, 2007.

[34] McDonarld, Dettwiler, and L. Associates, *Radarsat-2 Product Description*, May 2014.

[35] European Space Agency, Sentinel - 1 Team, *Sentinel-1 User Handbook*, 2013.

[36] W. Dan, P. LeDantec, M. Chabot, A. Hillman, K. James, R. Caves, A. Thompson, C. Vigneron, and Y. Wu, "RADARSAT-2 Image Quality and Calibration Update," June 3-5 2014.

[37] European Space Agency (ESA), *S-1A TOPS Radiometric Calibration Refinement*, 2015.

[38] Italian Space Agengy (ASI), *COSMO-SkyMed Mission and Products Description*, January 2014.

[39] M. Farge, "Wavelet transform and their applications to turbulence," *Ann. Rev. Fluid Mech.*, vol. 24, pp. 395–457, 1992.

[40] J. P. Antoine and R. Murenzi, "Two-Dimensional directional wavelets and the scale-angle representation," *Signal Processing*, vol. 52, pp. 259–281, 1996.

[41] J. P. Antoine, R. Murenzi, P. Vandergheynst, and S. Twareque Ali, *Two-Dimensional Wavelets and Their Relatives*. Cambridge University Press, 2004.

[42] H. Hersbach, A. Stoffelen, and S. de Haan, "An improved scatterometer ocean geophysical model function: CMOD5," *Journal of Geophysical Research*, vol. 112, pp. 5767–5780, 2007, (doi:10.1029/2006jc003743).

[43] X. M. Li and S. Lehner, "Algorithm for Sea Surface Wind Retrieval From TerraSAR-X and TanDEM-X Data," *IEEE Trans. Geos. and Remote Sensing*, vol. 52, no. 5, pp. 2928–2939, 2014.

[44] G. I. Taylor, "The Spectrum of Turbulence," *Proc. R. Soc. London, Series A, Mathematical and Physical Sciences*, vol. 164, no. 919, pp. 476–490, 1938.

[45] G. K. Carvajal, L. E. B. Eriksson, and L. M. H. Ulander, "Retrieval and Quality Assessment of wind velocity vectors on the ocean with c-band SAR," *IEEE Trans. Geos. and Remote Sensing*, vol. 52, no. 5, 2014.

[46] S. Zecchetto and F. De Biasio, "Sea surface winds over the Mediterranean Basin from satellite data (2000-2004): meso- and local-scale features on annual and seasonal timescales," *Journal of Applied Meteorology and Climatology*, vol. 46, no. 6, pp. 814–827, 2007.

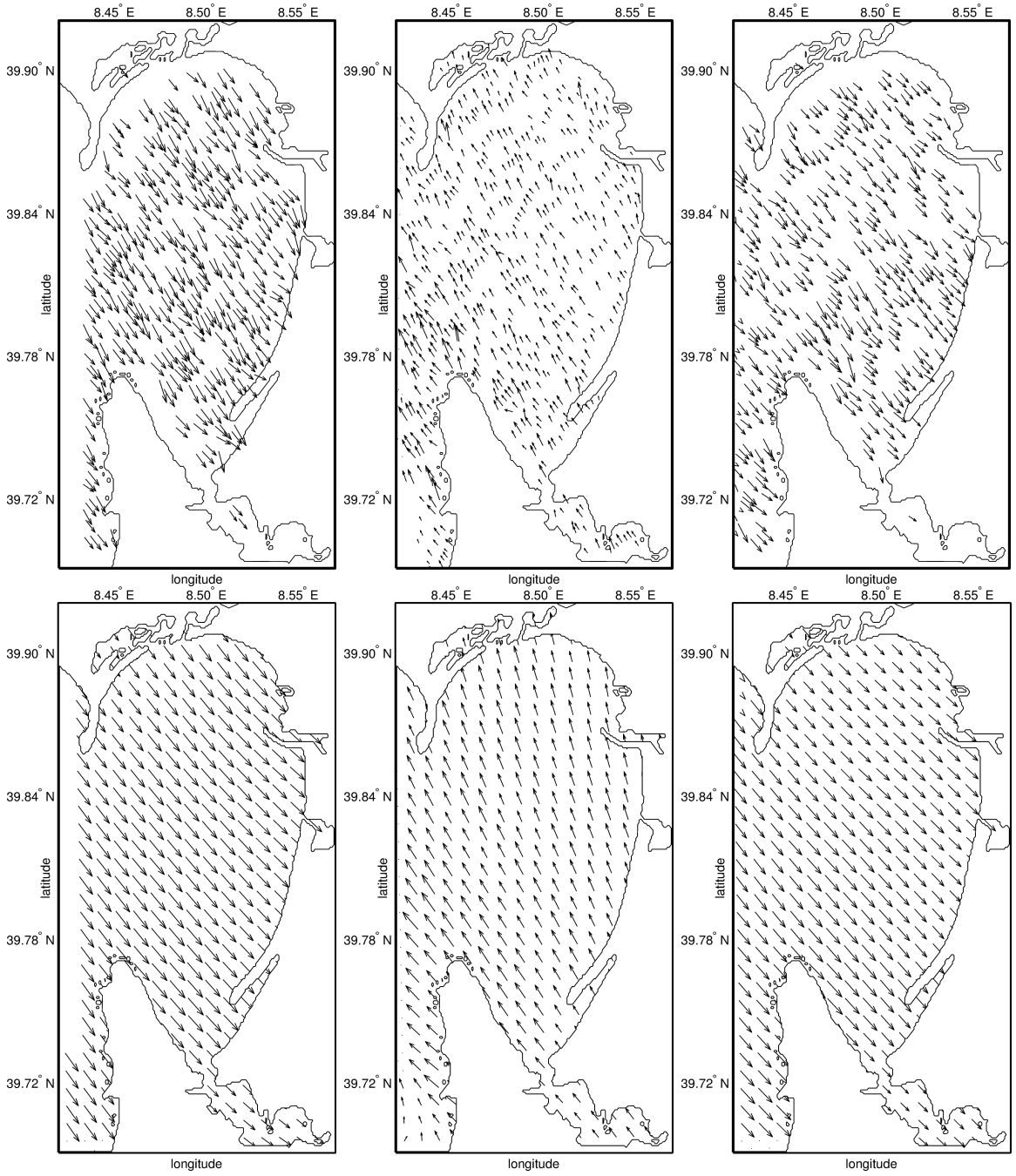

Fig. 4. The wind field obtained from the 2D-CWT technique applied to the SAR images of Fig. 2 (top panels) and from WRF atmospheric model (bottom panels). Left panels: COSMO-SkyMed. Middle panels: Radarsat-2. Right panels: Sentinel-1A.

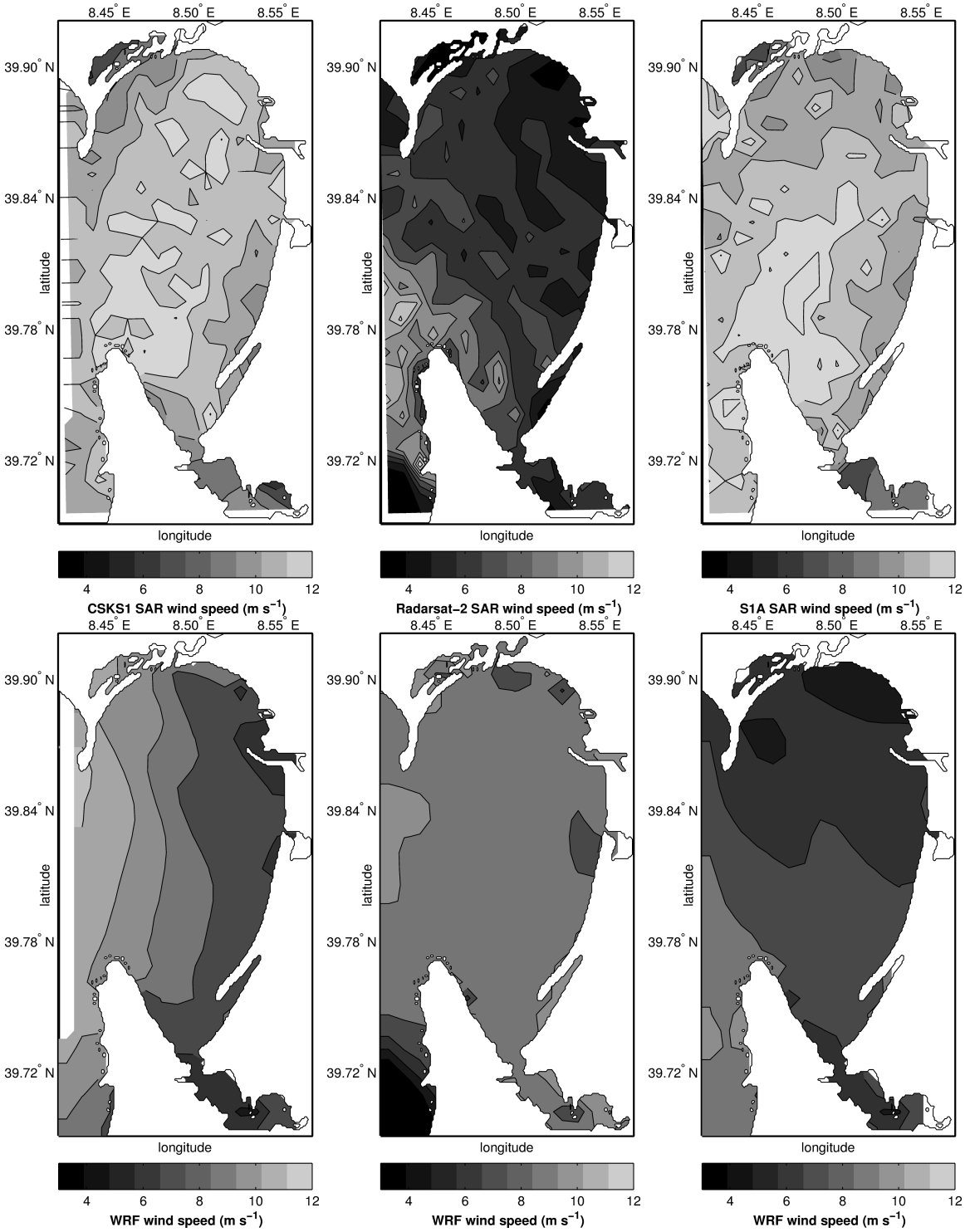

Fig. 5. Examples of wind speed field in the Gulf of Oristano. Top panels: from SAR. Bottom panels: from WRF model. Left panels: Cosmo-SkyMed; Middle panels: Radarsat-2; Right panels: Sentinel-1A.